GA–A23272

CONTROL OF THE RESISTIVE WALL MODE IN ADVANCED TOKAMAK PLASMAS ON DIII–D

by
A.M. GAROFALO, E.J. STRAIT, J. BIALEK, E. FREDERICKSON,
M. GRYAZNEVICH, T.H. JENSEN, L.C. JOHNSON, R.J. La HAYE, G.A. NAVRATIL,
E.A. LAZARUS, T.C. LUCE, M. MAKOWSKI, M. OKABAYASHI, B.W. RICE,
J.T. SCOVILLE, A.D. TURNBULL, M.L. WALKER, AND THE DIII–D TEAM

NOVEMBER 1999

DISCLAIMER

GA–A23272

CONTROL OF THE RESISTIVE WALL MODE IN ADVANCED TOKAMAK PLASMAS ON DIII–D

by
A.M. GAROFALO,* E.J. STRAIT, J. BIALEK,* E. FREDERICKSON,†
M. GRYAZNEVICH,◊ T.H. JENSEN, L.C. JOHNSON,† R.J. La HAYE, G.A. NAVRATIL,*
E.A. LAZARUS,‡ T.C. LUCE, M. MAKOWSKI,§ M. OKABAYASHI,† B.W. RICE,ƒ
J.T. SCOVILLE, A.D. TURNBULL, M.L. WALKER, AND THE DIII–D TEAM

This is a preprint of a paper to be presented at the 2nd IAEA Technical Committee Meeting on Steady-State Operation of Magnetic Fusion Devices, October 25–29, 1999, Fukuoka, Japan and to be published in the Proceedings

*Columbia University, New York, New York.
†Princeton Plasma Physics Laboratory, Princeton, New Jersey.
◊UKAEA-Culham Laboratory, Abingdon, United Kingdom.
‡Oak Ridge National Laboratory, Oak Ridge, Tennessee.
§Lawrence Livermore National Laboratory, Livermore, California.
ƒXenogen, Alameda, California.

Work supported by
the U.S. Department of Energy
under Contract Nos. DE-AC03-99ER54463, DE-AC02-76CH03093,
DE-AC05-96OR22464, W-7405-ENG-49, and Grant No. DE-FG02-89ER53297

GA PROJECT 30033
NOVEMBER 1999

ABSTRACT

Resistive wall mode (RWM) instabilities are found to be a limiting factor in advanced tokamak (AT) regimes with low internal inductance. Even small amplitude modes can affect the rotation profile and the performance of these ELMing H–mode discharges. Although complete stabilization of the RWM by plasma rotation has not yet been observed, several discharges with increased beam momentum and power injection sustained good steady-state performance for record time extents. The first investigation of active feedback control of the RWM has shown promising results: the leakage of the radial magnetic flux through the resistive wall can be successfully controlled, and the duration of the high beta phase can be prolonged. The results provide a comparative test of several approaches to active feedback control, and are being used to benchmark the analysis and computational models of active control.

1. INTRODUCTION

Operation with high values of β_N and of the bootstrap current fraction in both the advanced tokamak [1,2] and the spherical torus [3] requires stabilization of the low toroidal mode number *n* ideal magnetohydrodynamic (MHD) kink mode. (Here $\beta_N = \beta / (I / aB)$, $\beta = 2\mu_0 \langle p \rangle / B_0^2$, $\langle p \rangle$ is the volume averaged pressure, B_0 is the external toroidal field, I is the total toroidal current in MA, and a is the plasma minor radius.) A perfectly conducting wall placed close enough to the plasma can provide this required stabilization, thus offering the possibility of a compact and economical fusion reactor. In the presence of a real wall, the kink mode can persist as the resistive wall mode [4] (RWM), where the mode rotation and growth rate (f and γ, respectively) are limited according to: $f \le 1/2\pi\tau_w$ and $\gamma \le 1/\tau_w$, with τ_w the wall resistive decay time.

Recent theories [5,6] have predicted that the presence of dissipation in the plasma can stabilize the RWM at sufficiently high plasma rotation. However, the experiments reported in this paper confirm previous observations [7,8] that the plasma rotation always slows when $\beta_N > \beta_N^{\text{no wall}}$ ($\beta_N^{\text{no wall}}$ is the β_N limit predicted without wall stabilization). The toroidal rotation achieved in DIII–D plasmas does not seem to be sufficient to completely suppress the RWM. The destabilization of the RWM and its damping of the plasma toroidal rotation correlate with the saturation of the plasma β_N at a value near the limit calculated in absence of a conducting wall. In order to maintain $\beta_N > \beta_N^{\text{no wall}}$ active control of the RWM is needed.

Experiments on feedback stabilization of the RWM have begun [9] in DIII–D using the existing six-element error field correction coil (C–coil) and three new power amplifiers to apply an external n=1 radial magnetic field that is monitored by a toroidal array of sensor saddle loops located against the resistive wall. A qualitative survey of several feedback schemes has been carried out, with emphasis on the “smart shell” [10] and the “mode control” [11] concepts. The results show that the leakage of the n=1 flux through the sensor loops can be controlled, and the onset of the RWM induced beta collapse can be delayed. The experimental results are consistent with the simulations performed with the three-dimensional feedback modeling code VALEN, which predict only a small improvement in stability against the RWM with a feedback system using the present sensor and active coil geometry [12]. The VALEN code combines the electromagnetics code SPARK [13], an ideal MHD plasma model [14], and a model of an external feedback control coil system. VALEN modeling and analysis of the recent experimental results are being used to guide the design of extensions to the present feedback system that would further improve RWM stabilization.

2. MANIFESTATION OF THE RESISTIVE WALL MODE IN ADVANCED TOKAMAK OPERATING MODES

Earlier DIII–D experiments [8,12] aimed at studying the physics of the RWM have developed and utilized a target plasma with a very low β_N limit (~2) calculated without a wall for the n=1 ideal external kink. These single-null divertor target plasmas produced equilibria up to 40% above the no-wall β_N limit, and allowed reproducible observation of the RWM with moderate demands on the heating power. More recently, the RWM was observed in two new target plasmas which have the characteristics desired for advanced tokamak discharges: high normalized beta, high confinement, a large fraction of non-inductive current, and nearly steady-state plasma conditions.

The first of these regimes is a double-null, ELMing H–mode discharge with high q_{min} (~2), q_{95} ~4.5, and very low internal inductance ℓ_i ($\leq$ 0.7). The temporal evolution for one of these discharges is shown in Fig. 1. A small amplitude, nearly stationary and slowly growing n=1 mode is observed on the toroidal array of external saddle loops when β_N exceeds the value of 4 ℓ_i, which is an empirical scaling of the β_N limit for DIII–D discharges [15,16]. The no wall β_N stability limit to the n=1 ideal kink mode calculated by the GATO code [17] for this type of discharges is generally within 10% of the 4 ℓ_i value. By repeating the discharge with small variations of the plasma profiles, it was possible to rule out that the small n=1 perturbed radial field δB_r could simply be due to a pick up of axisymmetric field changes. The saddle loops also show a slow toroidal rotation of the mode (~2 Hz) in the direction of the electron diamagnetic drift (counter to the beam injection) while the plasma toroidal rotation measured from charge exchange recombination (CER) spectroscopy exceeds 4 kHz at the q=4 surface.

The n=1 mode is therefore identified as a RWM. The mode grows at a rate « $1/\tau_w$ often without causing a disruption, but always slowing down the plasma rotation across the entire minor radius. The time trace of β_N in Fig. 1 rolls over after the RWM onset, and falls back below 4 ℓ_i, at which time the growth of the RWM stops. The degradation in the energy confinement (note the increase in the D_α light emission baseline at mode onset) could be explained by either the reduced rotation and rotational shear [18], or formation of magnetic islands in some region of the plasma. The high density of this type of discharge prevents measurement of the electron temperature profile by electron cyclotron emission (ECE) spectroscopy to rule out the presence of magnetic islands, as was done in

Ref. [8]. The degraded confinement often limits β_N to just below the no-wall limit, or 4 ℓ_i where the RWM amplitude saturates at a small amplitude (1–3 Gauss). Note in Fig. 1 that the toroidal rotation recovers only when the saturated RWM δB_r amplitude disappears as β_N drops well below 4 ℓ_i.

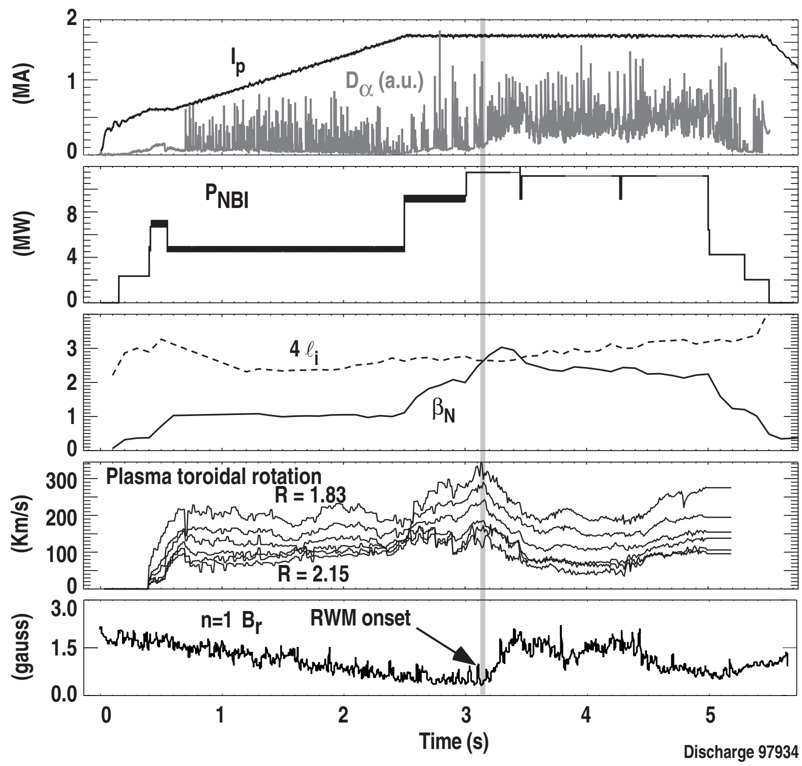

Fig. 1. The RWM provides a soft beta limit in these high q_{min}, low internal inductance, double-null discharges. Time evolution of (a) plasma current and divertor D_α emission, (b) neutral beam power, (c) normalized beta and four times the internal inductance, (d) toroidal plasma rotation, (e) n = 1 B_r amplitude measured outside the vessel (the slow ramp between t = 0 and t = 2.5 s is caused by residual pickup of axisymmetric field changes during the plasma current ramp up). Discharge 97934, B_t = 2.1 T, q_{95} ~ 4.5.

RWM instabilities were also observed in a second AT regime, a double-null, ELMing H–mode discharge with q_{min} ~1.7 and q_{95} ~ 5.5. The temporal evolution for two of these discharges is shown in Fig. 2. Operationally, the only difference between the two discharges is in the total power of injected neutral beams. The discharge with lower injected power, #98960, experiences a minor disruption at t = 1.8 s caused by an n=1 RWM that grows up to ~15 gauss at the wall, with growth rate ~$1/\tau_w$, and rotation rate ~5 Hz in the electron diamagnetic drift direction. β_N reaches ~3.6 with ℓ_i ~ 0.9 before the disruption. Ideal MHD calculations with the GATO code indicate that for these discharges the no wall β_N limit against the n=1 mode also coincides with 4 ℓ_i. Surprisingly, however, the discharge with higher injected power, #98976, did not show a more disruptive behavior on the way to a higher β_N. Instead, the high-performance phase was sustained for a longer duration with the value of β_N fluctuating around the value of 4 ℓ_i and with a complete absence of rotating MHD instabilities. The discharge maintained high normalized performance parameters of $\beta_N H_{89p} \geq 8$ for ~2 s, until the beam power was stepped down (H_{89p} is the energy confinement enhancement factor with respect to the ITER-89P L–mode confinement scaling [19]). Measurements of the internal loop voltage at this time show that about 75% of the plasma current is supplied noninductively, and more than 50% of the total current is calculated to be bootstrap current.

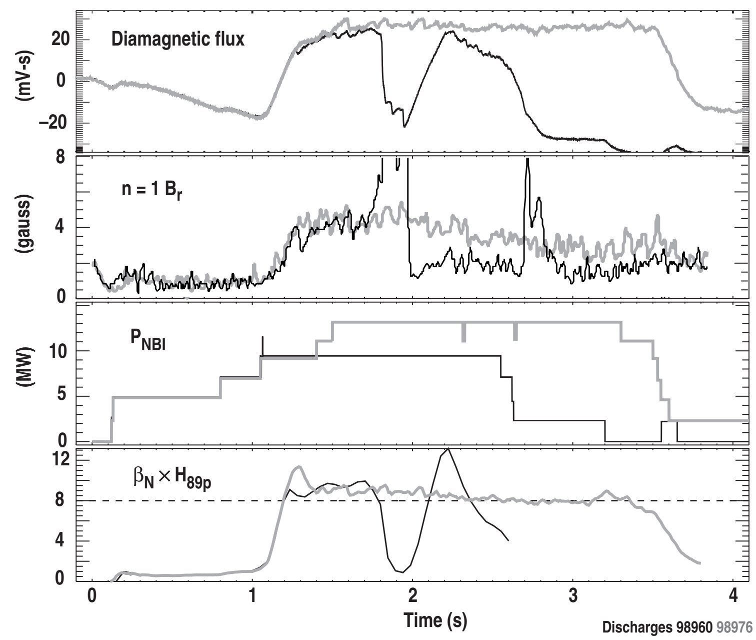

Fig. 2. Comparison of temporal evolution of two high performance, AT discharges with 10 MW (solid) and 13 MW (dotted) of neutral beam injected power, 98960 and 98976. (a) Diamagnetic flux; (b) n = 1 B_r amplitude at the vessel wall (the apparent increase between t = 1.0 and t = 1.2 s is caused by residual pickup of axisymmetric field changes during the rapid increase of stored energy at the L to H mode transition); (c) neutral beam power; (d) product of normalized beta and the energy confinement enhancement factor with respect to the ITER-89P L–mode confinement scaling. I_p = 1.2 MA, B_t = 1.6 T, q_{95} ~ 5.5.

All discharges in this regime show fluctuations in β_N that correlate with fluctuations in the n=1 δB_r from the saddle loop array and with fluctuations in the plasma toroidal rotation from CER spectroscopy. The correlation is shown clearly in the data from a similar discharge 100219 in Fig. 3. The n=1 δB_r grows and the edge plasma rotation

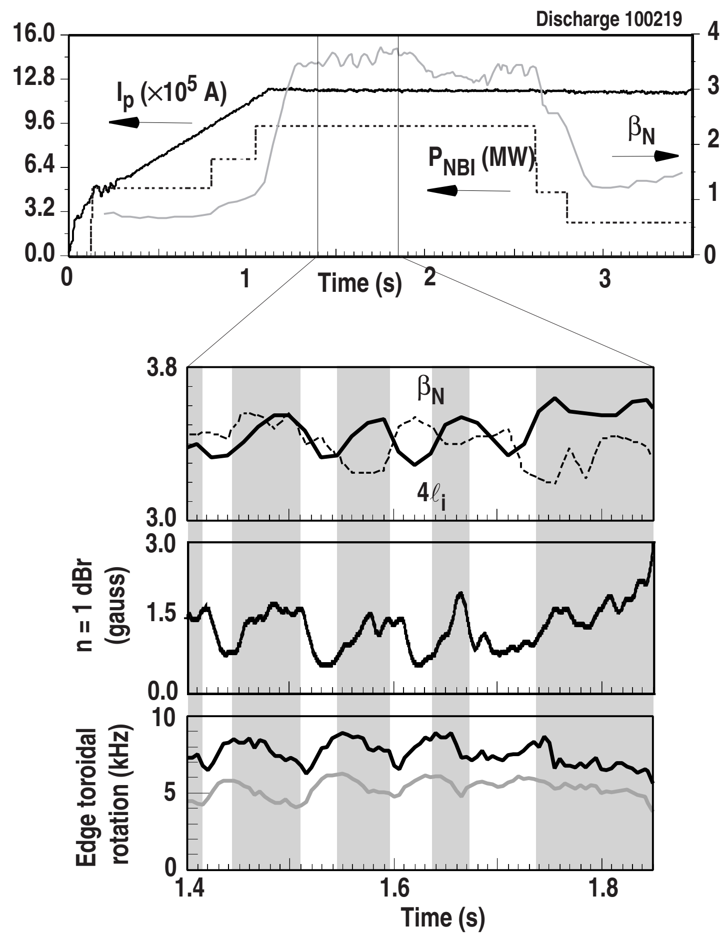

Fig. 3. Time evolution of high performance AT discharge 100219 (B_t = 1.6 T, q_{95} ~ 5.5). (a) Plasma current, neutral beam power and normalized beta. Time expansion of (b) normalized beta and four times the internal inductance; (c) n = 1 B_r amplitude of the RWM bursts; (d) plasma toroidal rotation at flux surfaces with q just below and q just above 3 (ρ ~ 0.8).

decreases while β_N is above 4 ℓ_i, until a collapse of the edge temperature temporarily reduces β_N below 4 ℓ_i. During the beta drop the n=1, δB_r decays and the plasma rotation promptly recovers. The fluctuations in the plasma rotation have an increasingly larger lag at smaller minor radius. Because these n=1 perturbations grow only when β_N is above $\beta_N^{\text{no wall}}$ and because they are stationary in the presence of rapid plasma rotation, we identify them as yet another manifestation, this time in bursts, of the RWM. The n=1 structure of the bursts is clearly shown in Fig. 4. The figure also shows that during the decaying phase, these modes rotate at a frequency f ~ 20 Hz ~ $1/2\pi\tau_w$ in the direction of the ion diamagnetic drift (the direction of the beam injection).

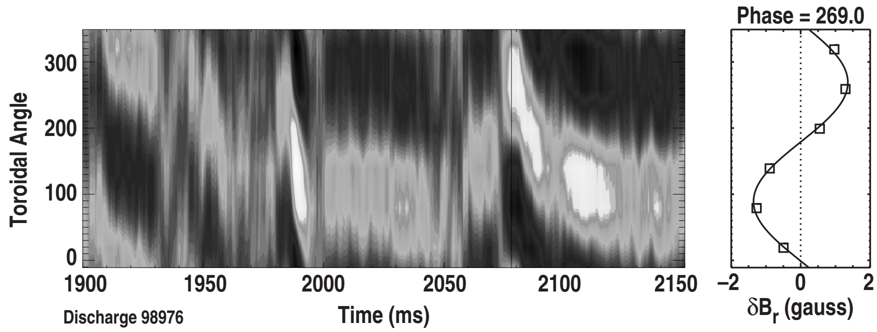

Fig. 4. (a) Color coded contour plot versus time and toroidal angle of the signals from the toroidal array of saddle loop sensors located outside the vessel, showing n = 1 structure and toroidal rotation of the instability bursts limiting β_N to just about 4 ℓ_i in discharge 98976. (b) Magnitude of the signals versus toroidal angle at t = 2.078 s.

It is not clearly understood why at some time one of these RWM bursts would grow to large amplitude and cause a disruption rather than continuing the small amplitude fluctuation as is shown in Fig. 2. However, it has been observed that these catastrophic occurrences are less frequent at higher injected beam power. Preliminary analysis of rotation profile measurements shows that discharges with higher injected beam power have a somewhat larger rotation rate at the plasma edge than discharges with lower beam power. Although unable to completely suppress the RWM, this higher plasma rotation may have had a mitigating effect on the mode growth when β_N is above $\beta_N^{\text{no wall}}$.

3. INITIAL RESULTS OF RESISTIVE WALL MODE FEEDBACK EXPERIMENTS

The results obtained so far from DIII–D experiments on wall stabilization imply that active control of the RWM is needed in order to maintain a steady-state value of β_N above $\beta_N^{\text{no wall}}$. Promising results have been shown in a previous open-loop experiment of active control of the RWM [20], which made use of a static n=1 magnetic field applied by the six-element error field correction coil (C–coil). The recent feedback experiments have used three new current-controlled, switching-power amplifiers with a frequency range of 0–100 Hz to energize the C–coil with a current of up to 5 kA. This current can produce an n=1 radial magnetic field of up to 50 Gauss at the vessel wall, although some of the coil pairs may require up to 2 kA of the available current for correction of the error field. The configuration of the active coils and the sensor loops is shown in Fig. 5. Most of the feedback results were obtained using the high performance AT discharges of Fig. 2 as target plasmas.

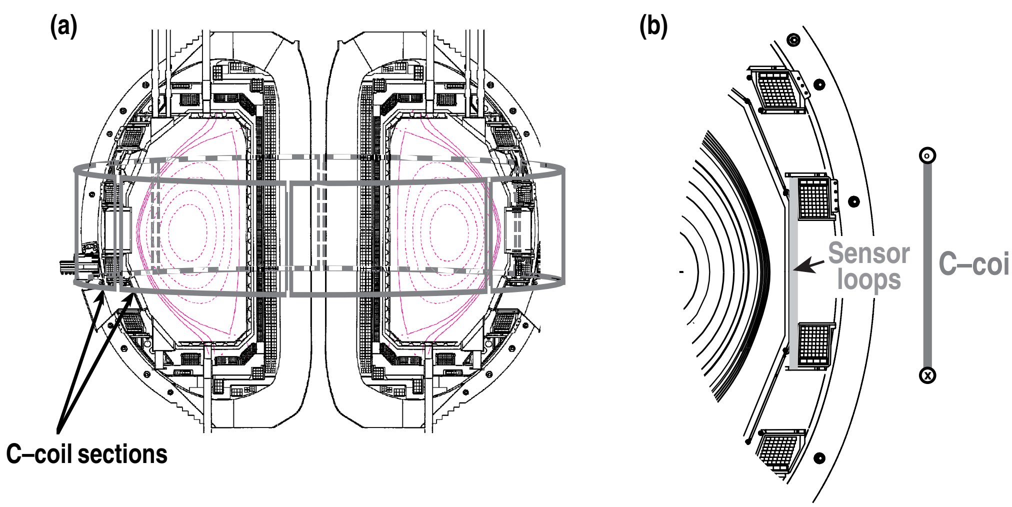

Fig. 5. Cross section of DIII–D showing (a) the six element error field correction coil (C–coil) used also as the active control coil for feedback stabilization of the RWM and (b) the location of the sensor loops.

For these initial experiments, the feedback system is designed to detect the amplitude and phase of an n=1 mode and to respond with an n=1 external field that opposes the mode; higher n modes are not considered. Let I_k be the current supplied by the feedback amplifier to the coil k. We can write for a generic feedback algorithm:

$$I_k \propto -G_P[B_r^{total} - \alpha B_r^{ext}](\phi_k + \delta\phi) - G_D \frac{d}{dt}[B_r^{total} - \alpha B_r^{ext}](\phi_k + \delta\phi),$$

where G_P and G_D are respectively the (real) proportional and derivative feedback gains, B_r^{total} is the total measured radial field at the vessel wall, and B_r^{ext} is the contribution from the external coils. The field B_r is evaluated at ϕ_k, the toroidal angle of coil k, plus a toroidal phase shift $\delta\phi$. The contribution B_r^{ext} is determined from the measured coil currents and mutual inductances of the coils and sensor loops. A qualitative survey of several feedback algorithms was carried out, with emphasis on the “smart shell” and the “mode control” concepts. In the basic implementation both algorithms use only proportional gain G_P in the closed loop system and aim at keeping null the radial field measured by the sensor loops. The “smart shell” scheme ($\alpha = 0$, $\delta\phi = 0$) mimics the magnetic properties of a perfectly conducting wall in the regions of the vessel that are covered by the sensor loops, by keeping the total (mode plus external) radial field in these regions equal to zero. In the “mode control” scheme (α=1, $\delta\phi$=0) the external field is subtracted (in hardware or software) from the sensor loop signals, so that the feedback current responds to the radial field amplitude from the RWM undiminished by the external field. Both algorithms can be modified by including a time derivative gain G_D. A spatial phase shift $\delta\phi$ can also be added between the feedback current and the measured field, which attempts to impart a stabilizing toroidal rotation to the RWM [21].

Figure 6 shows time traces of a basic smart shell algorithm experiment. The feedback system is clearly successful at keeping the n=1 saddle loop signals zero. The feedback currents respond to variations of the radial flux linked by the sensor loops compensating the leakage. Nevertheless, at about 1.42 s the feedback currents diverge, revealing that a mode is growing at finite rate. At t=1.48 s, during a more rapid mode rotation, the feedback is no longer able to keep a frozen flux at the sensor loops, and the mode starts growing more rapidly and through the wall, eventually causing a minor disruption.

Because in these discharges the RWM occurrences are not reproducible in onset time and effect, one cannot easily conclude whether the mode growth rate was slower than it would have been without feedback. We have therefore used a statistical approach in our analysis. The results are illustrated in Table 1. Significant improvements ΔT in the duration at high beta (defined as $\beta_N \geq 3.5\ \ell_i$) were observed for the “smart shell” algorithm with derivative gain (ΔT = 125 ± 70 ms) and the “mode control” algorithm with derivative gain (ΔT = 690 ± 430 ms). Some improvement in duration was also observed for the "mode control" algorithm with proportional gain only, and the "mode control" algorithm with a toroidal phase shift to drive rotation in the direction of the beam injection (co-rotation), but these results each represent only a single discharge and so cannot be considered statistically significant. For each discharge, the reference value T_0 selected for this statistical analysis was the median duration at high beta among discharges with same operational conditions but without feedback. Occasional discharges without feedback had longer duration, comparable to duration obtained with feedback, but these occurrences were rare. These experiments were deliberately conducted near the no wall stability limit, since modeling predicts that only a small improvement in maximum beta is possible with feedback control using the present (not optimized) coil set. The observations that occasional long duration discharges are obtained without feedback, but that the reliability improves with feedback, are consistent with operation near marginal stability.

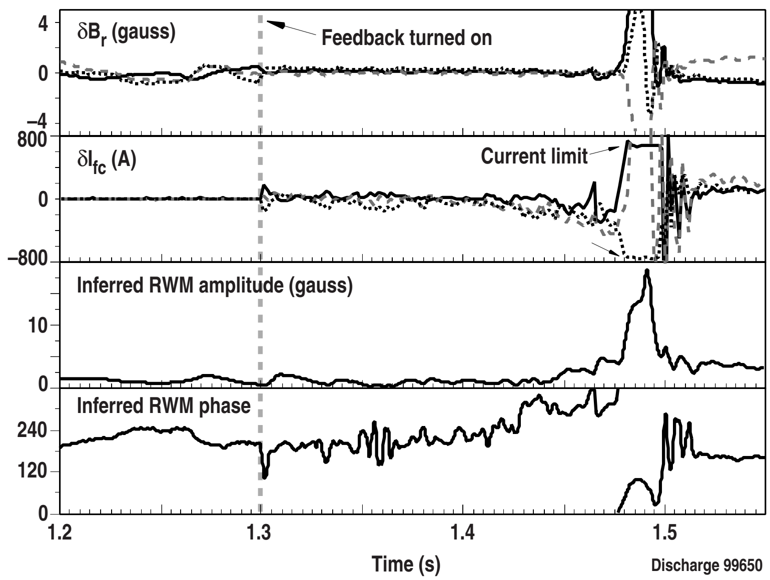

Fig. 6. Time evolution of a high performance discharge with "smart shell" feedback control of the RWM. (a) n = 1 component of the B_r measured by three opposing sensor loop pairs, (b) the three feedback coil currents, (c) n = 1 B_r amplitude of the RWM inferred from the opposing coil currents and the total measured B_r, (d) inferred toroidal phase of the RWM.

TABLE 1. INCREASE IN HIGH-BETA DURATION OBSERVED WITH VARIOUS FEEDBACK ALGORITHMS. THE TABULATED VALUES FOR EACH METHOD ARE THE MEAN DIFFERENCE IN DURATION FROM A REFERENCE VALUE, $\Delta T = T - T_0$, WITH THE STANDARD DEVIATION SHOWN FOR CASES WHICH WERE TRIED IN MORE THAN ONE DISCHARGE. THE REFERENCE VALUE T_0 IS THE MEDIAN HIGH-BETA DURATION WITH NO FEEDBACK, 390 MS FOR ONE SERIES OF DISCHARGES AND 610 MS FOR ANOTHER. THE "SMART SHELL" AND "MODE CONTROL" ALGORITHMS ARE EXPLAINED IN THE TEXT. SOME ALGORITHMS USED DERIVATIVE GAIN G_D IN ADDITION TO PROPORTIONAL GAIN, AS INDICATED. SOME ALGORITHMS INCLUDED A TOROIDAL PHASE SHIFT TO DRIVE MODE ROTATION, INDICATED HERE BY "CO" AND "COUNTER" RELATIVE TO THE DIRECTION OF PLASMA CURRENT AND NEUTRAL BEAM INJECTION.

Feedback Method	Improvement ΔT (ms)
Smart shell	–5 ± 124
Smart shell with GD	125 ± 69
Fake rotating shell Co	40
Fake rotating shell counter	–20 ± 14
Mode control	220
Mode control with GD	688 ± 426
Mode control Co	550
Mode control counter	0

4. SUMMARY AND CONCLUSIONS

Recent DIII–D experiments on steady-state AT target plasmas have shown how slowly growing or bursting RWMs can limit the value of β_N to approximately 4 ℓ_i (the no wall β_N limit). The plasma rotation is strongly reduced whenever a RWM amplitude is present, even if barely detectable by the sensor loops (resolution threshold ~1 Gauss). In the earlier experiments [8], a correlation between the plasma rotation slowdown and the value of β_N exceeding $\beta_N^{\mathrm{no\,wall}}$ was established. However, the presence of a RWM at finite amplitude during the slowdown was not always recognized. The data presented in this paper support the conclusion that the plasma rotation that has been achieved so far in DIII–D is not able to completely suppress the RWM, and the deceleration of the plasma rotation observed in the earlier experiments was caused by an undetected RWM with a saturated small amplitude or growing at a rate «$1/\tau_w$. In this paradigm the critical plasma rotation for destabilization of the RWM that was measured in previous experiments might actually mark a transition from saturation or slow growth to growth at a rate ~$1/\tau_w$. Whether the observation of growth rates «$1/\tau_w$ is consistent with any of the present linear theories, and how we can explain the saturation of the RWM amplitude when β_N decreases below $\beta_N^{\mathrm{no\,wall}}$ are new questions that will require further consideration.

Closed loop operation of a RWM feedback control system was carried out on high performance AT plasmas in DIII–D. Coupling of the feedback system to the MHD mode was demonstrated, and a modest extension of the average duration of the high beta phase was produced using the "mode control with time derivative gain" algorithm. The experimental results are consistent with the modest improvement in the beta limit predicted by the 3–D feedback modeling code VALEN with a feedback system using the sensors and active coils presently installed in DIII–D. Further investigation and optimization of the feedback circuit parameters are necessary. The results of this proof of principle experiment will be used to benchmark numerical models of the feedback stabilization process, such as the VALEN and PEST-VACUUM [22] codes. These codes can then be used as guidance in the design of an upgraded RWM feedback system that will be able to demonstrate sustained operation at β_N significantly exceeding $\beta_N^{\mathrm{no\,wall}}$ in a high performance AT scenario.

ACKNOWLEDGMENTS

This is a report of research sponsored by the U.S. Department of Energy under Contract Nos. DE-AC03-99ER54463, DE-AC02-76CH03093, DE-AC05-96OR22464, W-7405-ENG-49 and Grant No. DE-FG02-89ER53297.

REFERENCES

[1] A.D. Turnbull *et al*., Phys. Rev. Lett. **74** (1995) 718.

[2] C. Kessel *et al.*, Phys. Rev. Lett. **72** (1994) 1212.

[3] R.L. Miller *et al.*, Phys. Plasmas **4** (1997) 1062.

[4] J.P. Freidberg, *Ideal Magnetohydrodynamics*, Plenum Press, New York (1987).

[5] A. Bondeson and D.J. Ward, Phys. Rev. Lett. **72** (1994) 2709.

[6] R. Betti and J.P. Freidberg, Phys. Rev. Lett. **74** (1995) 2949.

[7] E.J. Strait *et al.*, Phys. Rev. Lett. **74** (1995) 2483.

[8] A. M. Garofalo *et al.*, Phys. Rev. Lett. **82** (1999) 3811.

[9] M. Okabayashi *et al.*, Proc. 25th EPS Conf. on Controlled Fusion and Plasma Physics, Maastricht, The Netherlands, 1999, Europhysics Conference Abstracts, Vol. 23J, p. 1661.

[10] C.M. Bishop, Plasma Phys. Controlled Fusion **31** (1989) 1179.

[11] M. Okabayashi *et al.*, Nucl. Fusion **38** (1998) 1607.

[12] A.M. Garofalo *et al*., Phys. Plasmas **6** (1999) 1893.

[13] D.W. Weissenburger, “Spark Version 1.1 User Manual,” Princeton Plasma Physics Laboratory Report PPPL-2494 (1988).

[14] A.H. Boozer, Phys. Plasmas **5** (1998) 3350.

[15] E.J. Strait *et al*., Phys. Plasmas **4** (1997) 1783.

[16] T.S. Taylor *et al.*, Plasma Phys. and Contr. Nucl. Fusion Research, Proc. 13th Int. Conf. Washington, D.C., 1990 (IAEA, Vienna, 1991), Vol. I, p. 177.

[17] L.C. Bernard, F.J. Helton, and R.W. Moore, Comput. Phys. Commun. **21** (1981) 377.

[18] L.L. Lao *et al.*, Phys. Plasmas **5** (1998) 1050.

[19] P.N. Yushmanov *et al.,* Nucl. Fusion **30** (1990) 1999.

[20] E.J. Strait *et al.*, in Plasma Phys. and Contr. Nucl. Fusion Research, Proc. 17th Int. Conf. Yokohama, Japan, 1998 (IAEA, Vienna, 1999); to be published in Nucl. Fusion (1999).

[21] R. Fitzpatrick and T.H. Jensen, Phys. Plasmas **3** (1996) 2641.

[22] M.S. Chance, Phys. Plasmas **4** (1997) 2161.